Computational Analysis Of Low Dimensional Magnetic Systems

Candidate Number: 601457
Project Number: CMP07
Supervisor: Prof. Stephen Blundell
Word Count: 6861

April 20, 2016

Abstract

This report will present the properties of low dimensional magnetic systems generated from computational methods. The spin-$\frac{1}{2}$ Heisenberg model is used to evaluate various one dimensional systems and the two dimensional layered chains, giving insight into how different configurations and magnetic coupling can influence the system's behaviour. Finite systems containing up to 12 atoms are studied and approximations are made for infinite atoms. The behaviour of the molecular magnet $CuCl_2(pyz)$ is modelled as a low dimensional system and compared with experimental data obtained from SQUID magnetometry. The g-factor and coupling constants were calculated as $g = 2.1(1)$, $J/k_B = -26.56(2)$K and $J_c/k_B = -8.01(5)$K which is in good agreement with other literature and demonstrates the effectiveness of the Heisenberg model with low dimensional approximations.

1 Introduction

This project involves the computational analysis of the magnetic and thermodynamic properties of molecular magnets constructed by N atoms. The fundamental properties of such systems can be understood by reducing the system to the molecular scale, whereby the atoms are modelled quantum mechanically as localised spins S that interact with each other magnetically and described under the spin-$\frac{1}{2}$ Heisenberg model.[1] The Heisenberg model is a simple yet effective method for approximating many-body systems that are coupled by magnetic interactions. Combining this with our knowledge of statistical mechanics allows us to generate the properties of the N-atom system.

This project will largely involve studying one dimensional spin-$\frac{1}{2}$ systems, which are much easier to work with than higher dimensions[2] and also extremely useful for modelling real magnetic structures such as ionic crystals. Such crystals have configurations similar to ionic chains, where the interaction between ions along the chain are strong but the interaction between chains are weak. For example, experimental evidence demonstrates how cupric quinone complex salts[3] have finite chains of 10 to 20 magnetic ions which can be modelled as a one dimensional Heisenberg system. Clearly there is much merit behind the computational analysis of one dimensional systems.

Python was used throughout this project with the NumPy and PyLab packages for mathematical operations and graph plotting. The project will first involve writing the code for the following steps:

1. Calculating the N-atom Pauli spin matrices for the Hamiltonian of system.

2. Solving for the eigenvalues for varying magnitudes of the external magnetic field, corresponding to all the possible energies of the system.

3. Creating the partition function of the system as a function of temperature.

4. Using the partition function to calculate the thermodynamic and magnetic properties of the system.

Computational modelling of one dimensional systems also provides the groundwork for more complex magnetic structures such as two dimensional layered systems and three dimensional networks. Some of these higher dimensional systems will be briefly studied in this project. Comparing the theoretical results with experimental measurements will allow us to confirm the effectiveness of the Heisenberg model for predicting the behaviour of magnetic systems. This report is structured as follows: theory and method are discussed in section 2, behaviour of various models are calculated and analysed in section 3, and then comparison with experimental results are made in section 4. The conclusions are presented in section 5.

2 Theory and method

2.1 Hamiltonian of the system

The project will model the atoms of the system as purely individual spin-$\frac{1}{2}$ objects interacting with each other under the Heisenberg Hamiltonian[1] given by

$$H = -\sum_{ij} J_{ij} \boldsymbol{S}_i \cdot \boldsymbol{S}_j - g\mu_{\mathrm{B}} \sum_{i=1}^{N} \boldsymbol{B} \cdot \boldsymbol{S}_i. \quad (1)$$

This is the generalised Hamiltonian of the system, where the localised spins $\boldsymbol{S}$ are defined by $\boldsymbol{S} = \frac{1}{2}\boldsymbol{\sigma}$, where $\boldsymbol{\sigma}$ are the atom's Pauli spin matrices of the N-atom system. g is the Landé g-factor and $\boldsymbol{B}$ is the external magnetic field. J_{ij} is the coupling constant that determines the interaction energy between ith and jth atoms.

Boundary conditions can be added to specify the atomic configuration and energies of the system can be found by solving for the Hamiltonian's eigenvalues which in turn allows us to construct the partition function.

2.2 Constructing the Pauli spin matrices for N-atom system

Finding the Hamiltonian requires knowledge of the N-atom Pauli spin matrices, bearing in mind that the form of these matrices change depending on the number of atoms in the system N. Therefore the initial step of the problem involves constructing the x, y and z components of these Pauli matrices. The general formulae used to construct these matrices for N-atoms are given by

$$\begin{aligned}
\sigma_j^x &= \mathbb{1}_2 \otimes \mathbb{1}_2 \otimes ... \otimes \overset{j-1}{\mathbb{1}_2} \otimes \overset{j}{\sigma^x} \otimes \overset{j+1}{\mathbb{1}_2} \otimes ... \otimes \mathbb{1}_2 \\
\sigma_j^y &= \mathbb{1}_2 \otimes \mathbb{1}_2 \otimes ... \otimes \overset{j-1}{\mathbb{1}_2} \otimes \overset{j}{\sigma^y} \otimes \overset{j+1}{\mathbb{1}_2} \otimes ... \otimes \mathbb{1}_2 \\
\sigma_j^z &= \mathbb{1}_2 \otimes \mathbb{1}_2 \otimes ... \otimes \overset{j-1}{\mathbb{1}_2} \otimes \overset{j}{\sigma^z} \otimes \overset{j+1}{\mathbb{1}_2} \otimes ... \otimes \mathbb{1}_2.
\end{aligned} \quad (2)$$

This involves taking the correctly ordered outer products of 2×2 dimensional identity matrices $\mathbb{1}_2$ and the 2×2 dimensional Pauli spin matrices σ^x, σ^y and σ^z in different orders depending on the jth spin matrix being calculated. The j, $j-1$, $j+1$ above σ and $\mathbb{1}_2$ in equation (2) indicates their corresponding position in the calculation.

These matrices are $2^N \times 2^N$ dimensional matrices since they are created from N outer products of 2×2 dimensional matrices. This allows us to assemble the Hamiltonian from equation (1) which is essentially a linear combination of spin matrices. Notice that the Hamiltonian will also be a $2^N \times 2^N$ matrix with 2^N energy eigenvalues. So for 12-atoms, this requires the storage and manipulation of 4096×4096 dimensional matrices. As N is increased, a larger computational runtime is required. Thus the results of this project will be limited to the calculation of 12 atoms at most due to computational constraints.

2.3 Statistical mechanics to deduce properties of the system

Once the energy eigenvalues of the Hamiltonian are found, the methods of statistical mechanics can be implemented to calculate useful information about the system. The canonical ensemble is used by assuming that the system is in thermal contact with its environment at temperature T with a fixed number of atoms and volume. The properties at thermal equilibrium can be described with the 2^N energy eigenvalues ϵ_i from the Hamiltonian of the system by substituting them into the partition function Z given by

$$Z = \sum_{i}^{2^N} e^{-\beta\epsilon_i}, \quad (3)$$

where $\beta = (k_B T)^{-1}$.

The partition function can then be manipulated to produce various features of the system such as the free energy F, which in turn can be used to calculate magnetic properties such as the magnetic moment m and susceptibility χ. These are given by the following equations,

$$\begin{aligned}
F &= -k_{\mathrm{B}} T \log Z \\
m &= -\Big(\frac{\partial F}{\partial B}\Big)_T \\
\chi &= \lim_{H \to 0} \frac{m}{H} \sim \frac{m}{B/\mu_0},
\end{aligned} \quad (4)$$

where this expression for χ is valid in small fields ($\chi \ll 1$, so $B \sim \mu_0 H$). Similarly the thermodynamic variables such as the internal energy U can be found to calculate the heat capacity C of the system, which are given by

$$\begin{aligned}
U &= -\frac{\partial \ln Z}{\partial \beta} \\
C &= \frac{\partial U}{\partial T}.
\end{aligned} \quad (5)$$

These variables are most effectively calculated in the programme by using numerical approximations (see Appendix A). Once the correct code and results are generated, graphs illustrating the system's characteristics can be made. These are all the steps that need to be made to evaluate the properties of different atomic configurations.

3 Results and Analysis

3.1 Antiferromagnetic Rings

The first configuration that is considered will be the simplest case, which is the antiferromagnetic

ring. This is a chain of N atoms constructed into a ring interacting with antiferromagnetic coupling (see figure 1a). When evaluating a distinct atomic configuration, boundary conditions are added to the generalised Hamiltonian of equation (1), so the Hamiltonian is now given by

$$H = -J\sum_{i=1}^{N} \boldsymbol{S}_i \cdot \boldsymbol{S}_{i+1} - g\mu_B B \sum_{i=1}^{N} S_i^z, \qquad (6)$$

where i and $i+1$ indicate that only interactions with nearest neighbour spins have significant interaction energies. Periodic boundary conditions are imposed, $N+1=1$, creating a ring configuration. The external magnetic field B is projected along the z-axis. Antiferromagnetic conditions are held such that the coupling constant is negative and the same for all interactions, $J<0$. As a result, neighbouring spins have the lowest energy when they are anti-aligned to each other (satisfying Hund's rule) and the external field. For these calculations the value of the coupling constant used is $J/k_{\mathrm{B}} = -5\mathrm{K}$.

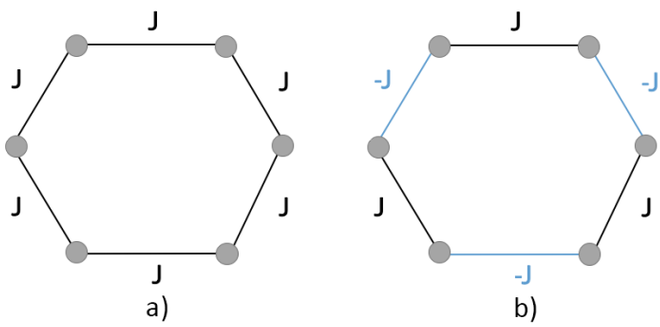

Figure 1: 5 atom ring systems a) constant coupling between each each neighbour b) alternating coupling between each neighbour

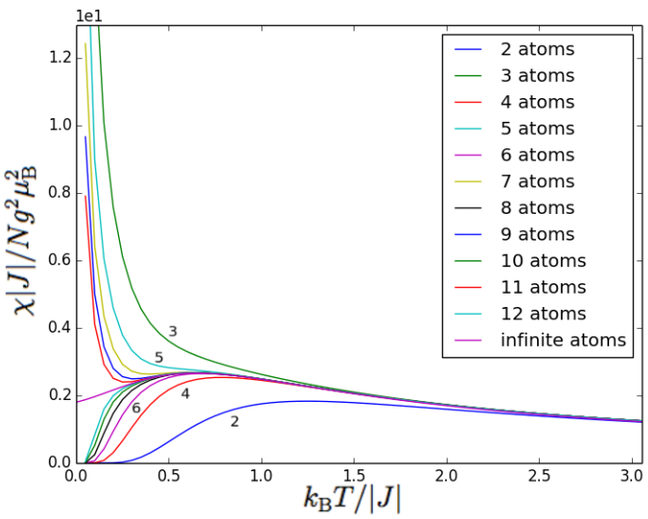

Figure 2: Magnetic susceptibility against temperature for antiferromagnetic Heisenberg rings with $N = 2, 3, ..., 12$ and ∞ atoms, given in dimensionless units of $\chi|J|/Ng^2\mu_{\mathrm{B}}^2$ versus $k_{\mathrm{B}}T/|J|$. (Numbers are included with plots to avoid confusion with similar colours).

The susceptibilities generated in Figure 2 agree well with previous simulations.[4] The plot for the infinite spin system is generated from the equation[5] given by

$$\chi = \frac{Ng^2\mu_{\mathrm{B}}^2}{k_{\mathrm{b}}T} \frac{0.25 + 0.074975x + 0.075236x^2}{1 + 0.9931x + 0.172135x^2 + 0.757825x^3} \qquad (7)$$

where $x = |J|/k_{\mathrm{b}}T$.

It is clear that the susceptibilities of odd and even N atom rings have distinctive properties. As temperature approaches zero, the susceptibility for even N rings approaches zero and diverges towards infinity for odd N rings. At high temperatures, all the curves begin to overlap and fall to zero asymptotically. These results can be intuitively explained by our understanding of magnetism and quantum mechanics.

The behaviour of odd N systems can be illustrated by evaluating the energies of the 3 atom ring which are shown in figure 3. At low temperatures,

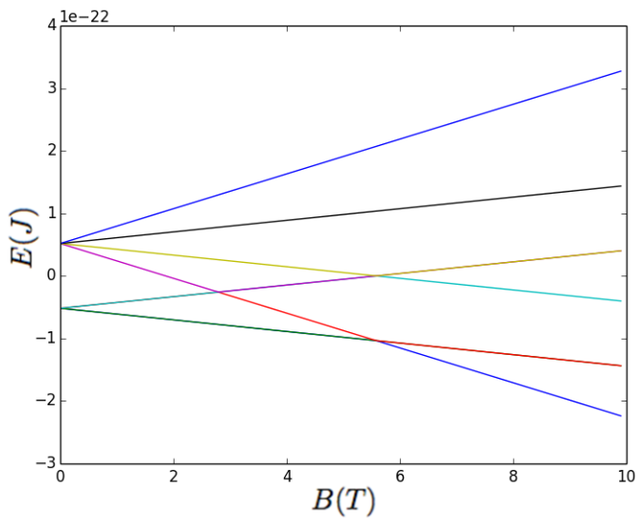

Figure 3: Energies of antiferromagnetic $N = 3$ system against external magnetic field.

electrons occupy the lowest energy states, which are the $S = \pm\frac{1}{2}$ states. These are the ground state energies that exists for all odd N systems. As these energies have a B field dependence, they will give rise to a magnetisation m with a $1/T$ dependence described by Curie's law. As the $1/T$ dependence from m is clearly unaffected when calculating χ (see equation (4)), this property is passed onto the magnetic susceptibility χ. At low temperatures, the $1/T$ dependence of χ causes a divergence towards infinity, and at high temperatures χ converges towards zero. Hence, this explains the behaviour of odd N susceptibilities at both low and high temperatures.

Similar reasoning can be used to explain the even N systems, illustrated best by analysing the energies of the 2 atom rings shown in figure 4.

At low temperature, electrons will occupy the lowest energy states, which is the $S = 0$ state for all even N systems. All of the electrons will occupy

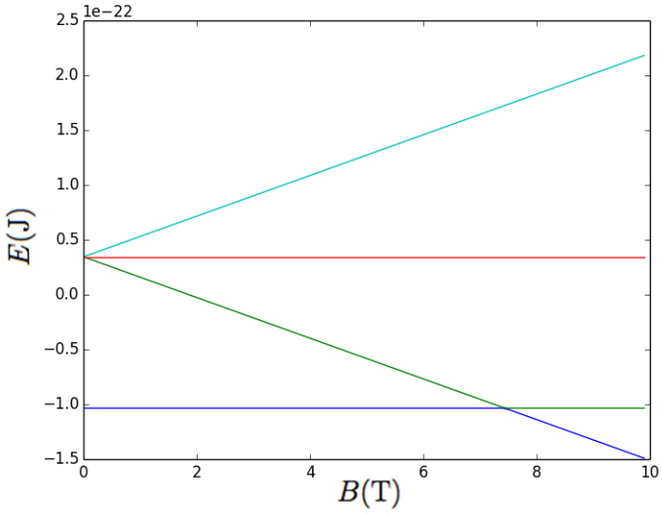

Figure 4: Energies of antiferromagnetic $N = 2$ system against external magnetic field.

this ground state, as there is not enough energy to occupy the higher energy states with B field dependences. Since this energy state is constant and clearly has no B field dependence, the magnetic moment and therefore the susceptibility will be negligible at very low temperatures. As the temperature increases, electrons will begin to occupy higher energy levels that have B field dependences, giving rise to non-zero susceptibilities.

At high temperatures for both odd and even N the curves begin to overlap in figure 2. This temperature provides enough energy for a much larger proportion of electrons to occupy the highest energy states with B field dependences, resulting in a weighted distribution of χ that has strong $1/T$ behaviour.

At intermediate temperatures, the electrons will begin to have enough energy to occupy higher energy states although the majority of the electrons still remain in the ground state. For even N rings, these higher energy states, unlike the ground state, have B field dependences (see figure 4). The susceptibilities are averaged between electrons in the ground states and the electrons in higher energies, giving a non-zero distribution for χ. This averaging also happens for odd N rings, where in this case all energy states, both ground and excited, will give rise to Curie law dependences with varying magnitudes. Around $k_{\mathrm{B}}T/|J| \sim 0.5$ a maximum/minimum will present itself from the averaged distribution of χ from the ground and excited states.

Other thermodynamic properties of the system can also be calculated such as the internal energy U and the heat capacity C by using the equations given in equation (5). Figure 5 shows how the odd and even N systems form two distinctly different behaviours, where the even N converges towards some sort of infinite N limit from below and the odd N from above. The even rings are always lower in energy than the odd rings because of the $S = 0$ ground state. As N increases, the ground states become lower in energy, but not proportionally to N, so the internal energy per atom for each N converges appropriately towards the infinite limit. The infinite limit has been further investigated by Bonner and Fisher.[4] At the high temperature limit, all N systems go towards zero as there is enough energy for electrons to occupy all states which cancel each other out.

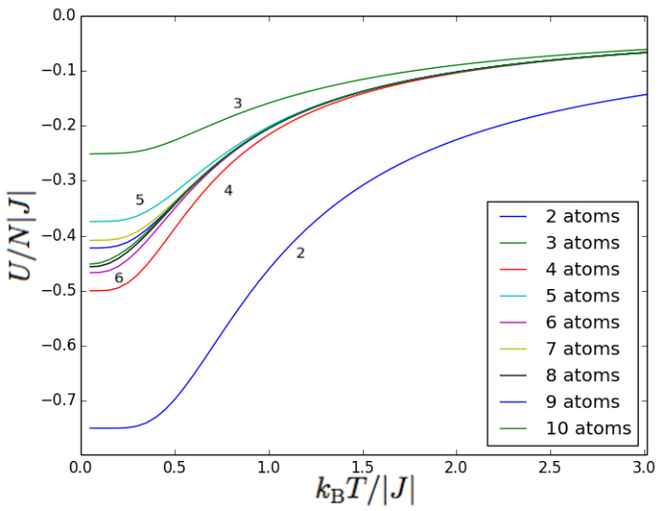

Figure 5: Variation of internal energy with temperature for antiferromagnetic Heisenberg rings with $N = 2, 3, 4, ..., 10$ atom rings given in dimensionless units of $U/N|J|$ against $k_{\mathrm{B}}T/|J|$.

The heat capacities are displayed in figure 6, where the convergence behaviour appears again. This time, the odd N systems converge towards an infinite limit from below and even N systems from above. This is not surprising as C is the gradient of U against T, and we can see from figure 5 that the gradients are larger for the even N than for the odd N. So all even N will have larger heat capacities than odd N which all converge towards an infinite limit. The peaks of the heat capacities are at different temperatures because the finite energy gap between the ground state and first excited states vary with N. As N increases, the energy gap is reduced which shifts the heat capacity peaks towards the infinite limit.

These results show that the Heisenberg model is extremely good for finding the behaviour of simple magnetic systems. This can now be altered to accommodate for different atomic configurations giving more insight into the behaviour of such magnetic systems.

3.2 Ferromagnetic Rings

There is much that can be deduced from making small modifications to the system, firstly a very basic change to the system is made by analysing the ferromagnetic rings. This Hamiltonian is identical to that of equation (9) with the same boundary conditions, the only change is that the coupling

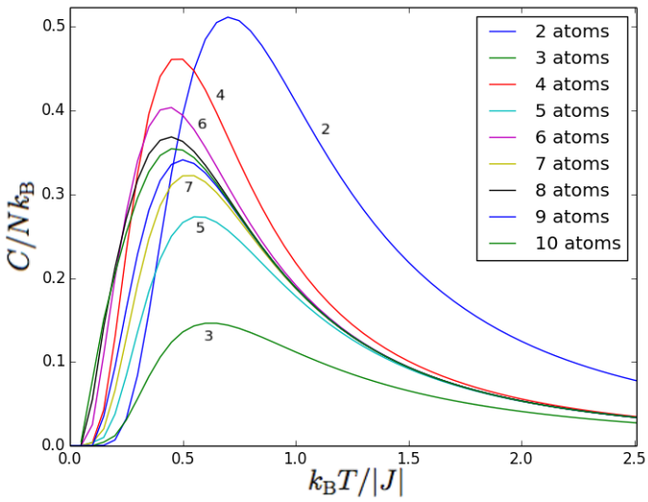

Figure 6: Heat capacity against temperature for antiferromagnetic rings with N $= 2, 3, ..., 11$ atom rings. These results are in dimensionless units of C/Nk_B and $k_BT/|J|$.

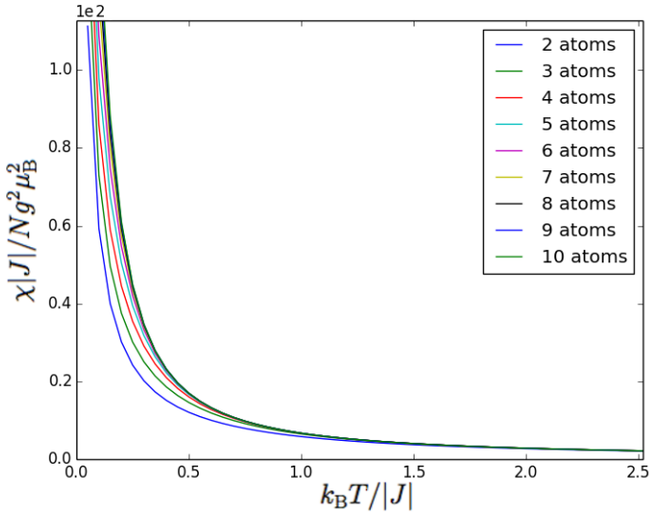

Figure 8: Magnetic susceptibility against temperature for ferromagnetic rings with $N = 2, 3, ..., 10$ atoms, given in dimensionless units.

constant J is now positive, $J > 0$, with the same magnitude. Neighbouring spins now have lowest energy when they are aligned to each other.

Figure 7 shows how this causes an inversion in the energies of the system. The lowest energy state now has a B field dependence, so all N atom systems act similarly to odd N antiferromagnetic systems at low temperatures. As the temperature increases, the system continues to display odd N behaviour due to the weighted averaged of the susceptibilities. This causes the susceptibility for all N to have $1/T$ dependence for all temperatures as shown in figure 8.

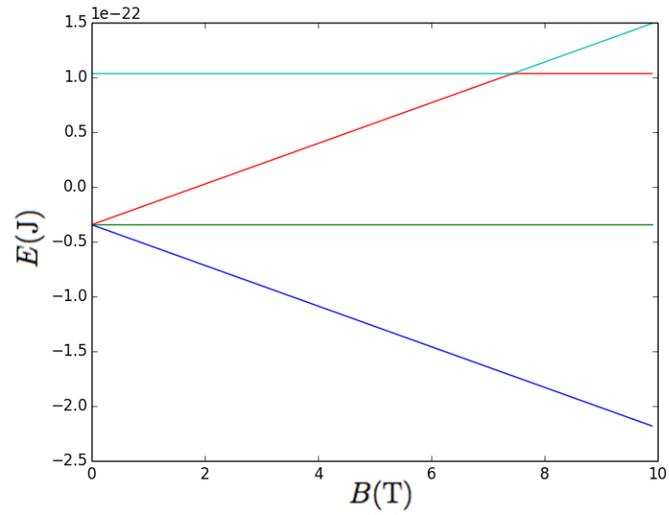

Figure 7: Energies of ferromagnetic $N = 2$ system against external magnetic field.

This happens to all even N energies, where the field independent $S = 0$ ground state becomes the highest energy state. The energy states of odd N systems will also be inverted but all of these states have B field dependences anyway so the general χ behaviour will remain the same. As a result of the energy inversion, both even and odd N ferromagnetic systems will have B field dependent ground states that gives rise to the $1/T$ dependence of susceptibilities.

3.3 Alternating Heisenberg Rings

Now that the basic system has been calculated and minor modifications have been successfully made for the ferromagnetic rings, larger changes can be made to the code to investigate more complicated systems. Much research has been conducted around systems with alternating magnetic behaviour[6,7] where crystalline solids[8] and inorganic molecular magnets[9] can be modelled as alternating one dimensional chains. Hence it will be useful to evaluate the behaviour of alternating rings (see figure 1b). Changing the boundary conditions of the generalised Hamiltonian in equation (1) will give the new Hamiltonian

$$H = -J\sum_{i=1}^{N/2}(\boldsymbol{S}_{2i}\cdot\boldsymbol{S}_{2i+1} - \boldsymbol{S}_{2i-1}\cdot\boldsymbol{S}_{2i}) - g\mu_B B\sum_{i=1}^{N} S_i^z. \tag{8}$$

Here the interaction along the ring changes successively from antiferromagnetic to ferromagnetic coupling, where the change of sign in the spin interactions imply the change in coupling between each neighbouring atoms. Only nearest neighbour interactions have a significant contribution to the energy of the system. The magnitude of the coupling constant J remains the same and only the sign changes. The magnetic field is still projected along the z-direction and the $N + 1 = 1$ condition remains to maintain a ring system.

The results in figure 9 shows the susceptibility for alternating rings with $|J|/k_B = 5$K. By comparing figure 9 and figure 2 we can see the difference in susceptibilities between the alternating and antiferromagnetic rings. The behaviour at very low and

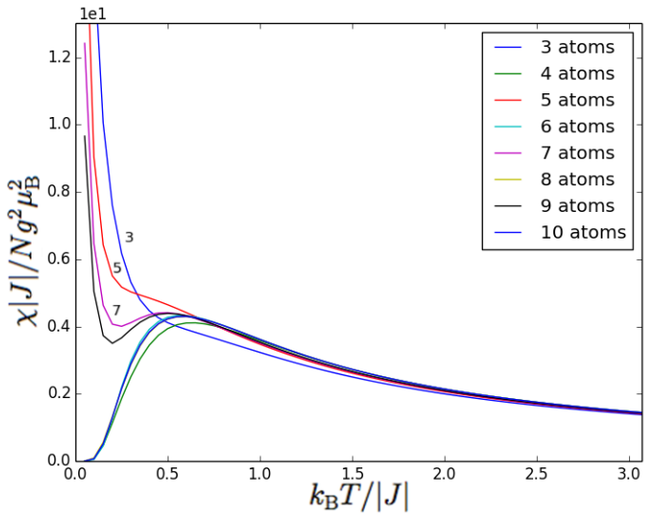

Figure 9: Magnetic susceptibility versus temperature for alternating Heisenberg rings with $N = 3, 4, ...10$ atoms, given in dimensionless units.

high temperatures are very similar, which can be explained with the same reasoning in Section 3.1. The main differences are at the intermediate temperatures, where the maximums of the alternating case around $k_BT/|J| \sim 0.5$ are larger by a factor of 2. Larger susceptibilities indicate the presence of more energy levels with field dependences, this is best seen by evaluating the differences in the energies of the two systems.

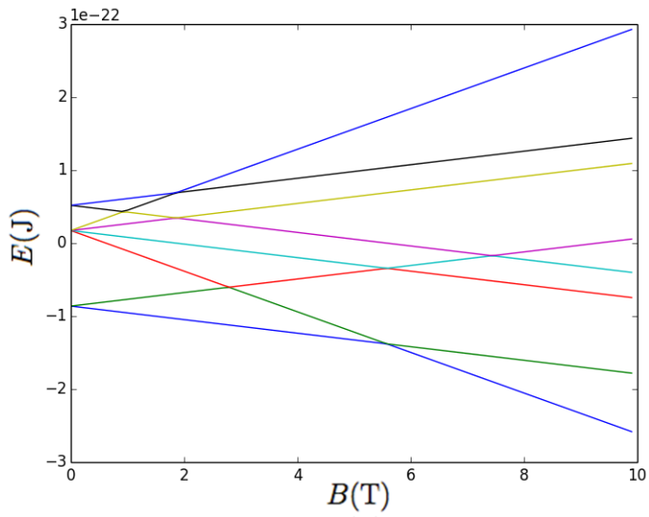

Figure 10: Energies of alternating $N = 3$ system against external magnetic field.

The energies from figure 10 and figure 3 are both for 3-atom rings but in different systems. There are 2 additional larger energy states in the alternating ring system. So as the temperature rises, there are larger energy states that can be occupied contributing to the rise in the average susceptibility. This difference applies for all N-atom rings in the alternating case, causing a rise in the weighted distribution of susceptibilities at intermediate temperatures.

3.4 Anisotropic Rings

So far we have been studying the Heisenberg model with all components of the spins interacting without any directional dependence. It would be interesting to see how the system behaves once an energetically favourable direction for spontaneous magnetization is imposed and then gradually lifted. Much theoretical study has been made on anisotropic rings[10] where the Hamiltonian is given as

$$H = -J\sum_{i}^{N}[S_i^z \cdot S_{i+1}^z + \alpha(S_i^x \cdot S_{i+1}^x + S_i^y \cdot S_{i+1}^y)] - g\mu_B B\sum_{i}^{N} S_i^z. \tag{9}$$

The nearest neighbour antiferromagnetism and the $N+1 = 1$ boundary condition remains, making the system an N-atom ring. The difference now is that there is an anisotropy factor α in front of the x and y components of the spins S. The anisotropy factor can be varied to show the behaviour of the system at different levels of α between 0 and 1. The Ising case corresponds to $\alpha = 0$ where only interactions along the z-direction are energetically favourable and $\alpha = 1$ corresponds to the Heisenberg case that we have been studying.

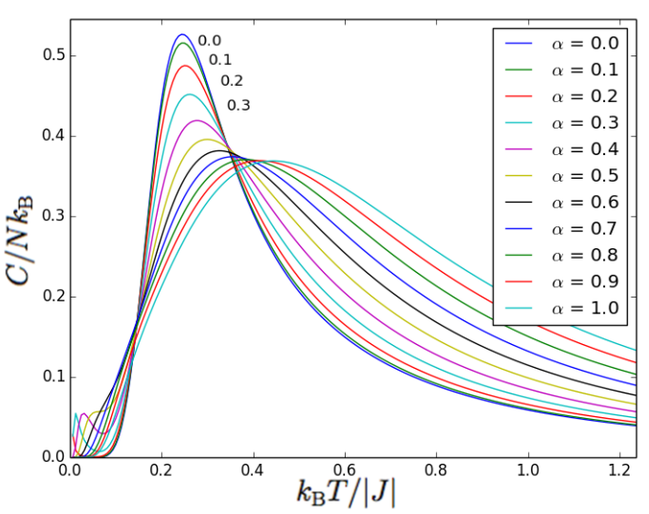

Figure 11: Heat capacities against temperature for an $N = 8$ system with changing α from 0 to 1 at intervals of 0.1, given in dimensionless units.

The specific heat capacities C for the 8 atom ring with changing α is shown in figure 11, generated with coupling $J/k_B = -5$K. At the high T limit, electrons will occupy all excited states, so no change in energy takes place causing C to converge to zero. As α increases from 0 to 1 the maximum broadens its peak, reduces its height, and shifts towards higher T. This can be most easily explained by observing how the energies change with α shown in figure 12.

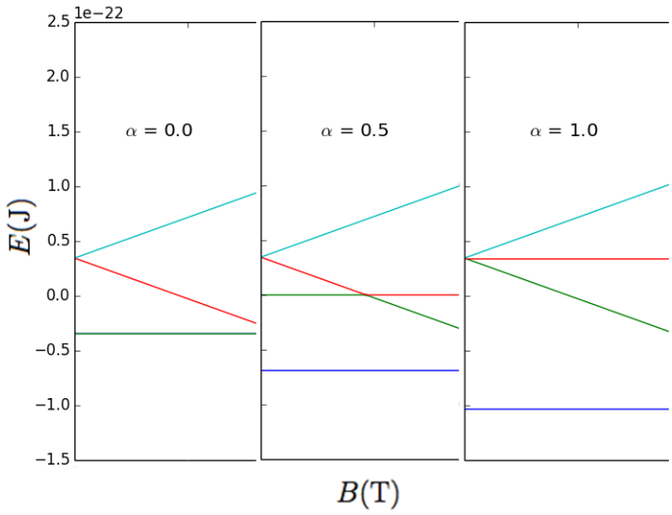

Figure 12: The energies of the $N = 2$ system against external magnetic field with anisotropy factor $\alpha = 0.0$, $\alpha = 0.5$ and $\alpha = 1.0$.

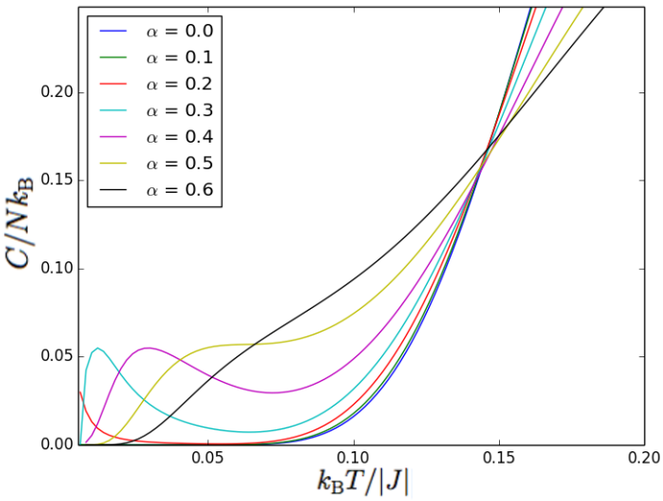

Figure 13: Heat capacities against temperature for the $N = 8$ system with $\alpha = 0.0 - 0.6$ at low temperatures, given in dimensionless units.

As α increases from 0 to 1 for the 2 atom system, the degenerate $S = 0$ ground states separate into distinctive energy levels. This degenerate energy splitting of the ground state due to the increase of α applies for all N atom systems.

For lower α $(0 - 0.5)$ the ground state begins to split, with one level increasing in energy and the other lowering in energy. The energy gap between the ground state and highest energy states are still much smaller than that for $\alpha = 1.0$. The smaller energy gap means that most electrons will be able to occupy higher energies at lower T causing a larger change in average U. Since C is the change in internal energy U with respect to T (see equation (5)), this gives a higher heat capacity peaks at lower T than that for larger α.

At high α $(0.6-1.0)$ the energy splitting is larger, so a larger T is required to excite electrons causing the C peaks to shift towards higher T. The peaks are now broader and lower because there are more excited states closer to each other due to the splitting (see figure 12 $\alpha = 1.0$), so the increase in T will allow electrons to occupy higher energy states, although the average change in U is reduced.

Although the most interesting results occur at the low temperature limit $(k_bT/J \sim 0.0 - 0.1)$ where the curves for even N rings with $\alpha = 0.2-0.5$ display small peaks and even points of inflection (see figure 13). This unusual behaviour is called the Schottky anomaly,[11] where the system behaves like an ideal paramagnet with two energy levels. This can be explained by observing the energies in figure 12 again. As α increases, the degenerate ground state begins to split which creates a very small energy gap. At low temperatures electrons can only occupy these two energies, which causes the small C peak to appear. At high α the splitting becomes much larger so small peaks do not appear as much larger temperatures are now required to excite electrons.

The heat capacity falls after the small peak around $k_bT/J \sim 0.0-0.05$ as the further increase in temperature is not enough for electrons to occupy even higher energy states so there is no change in average internal energy. In some cases ($\alpha = 0.5$) a point of inflection is produced as the larger splitting means that the higher energy from splitting is closer to the higher energy states. The further increase in temperature allows the electrons to occupy even larger energy levels, hence no drop in C occurs. So these thermodynamic properties at low temperature arise because of the way degenerate energies of the system splits due to the change in α.

The behaviour of the susceptibility due to changing α shown in figure 14 can also be explained by considering the change in energies shown in figure 12. As α increases, the peak of χ lowers itself, broadens and shifts slightly forward in temperature. We can see from figure 12 that the splitting of the ground state is very small at low α and larger apart for high α. So the peak will be pushed forward with increasing α as larger temperatures are required to excite the electrons. The excited energy states become closer together with increasing α, so peaks are broadened and lowered as a result of the averaged distribution of susceptibilities from the closely packed excited states.

3.5 Layered Chains

As mentioned in the introduction, the code written for the basic Heisenberg ring can provide the groundwork for more complex magnetic structures. Here we will investigate the properties of 2 dimensional layered chains (see figure 17), where there are nonzero interaction between each chain of atoms which creates a two dimensional plane of layered chains. This is extremely useful for modelling vari-

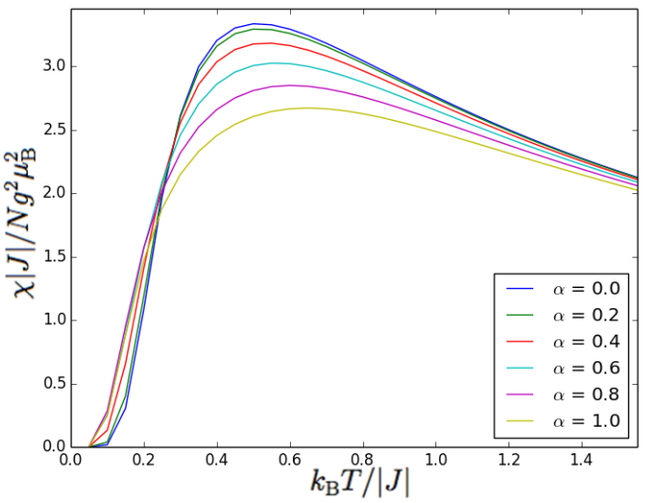

Figure 14: Magnetic susceptibility against temperature for the $N = 8$ system with changing α from $0.0 - 1.0$, given in dimensionless units.

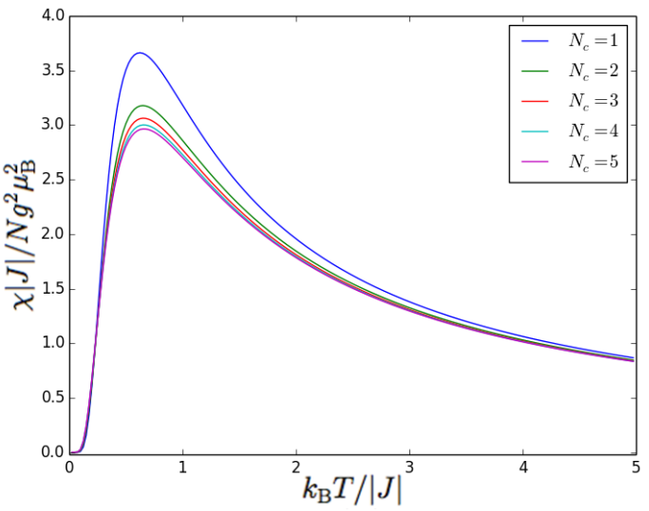

Figure 15: Magnetic susceptibility against temperature of layered systems with $1-5$ chains consisting of 2 atoms per chain, given in dimensionless units.

ous compounds such as BEDT-TFF salts,[12] where approximations can be made to ignore the interactions perpendicular to the plane reducing the system from 3 to 2 dimensions.[13] The Hamiltonian for the layered system is given by:

$$H = -J \sum_{\substack{\text{chain} \\ <i,j>}}^{N_c} \boldsymbol{S}_i \cdot \boldsymbol{S}_j - J_c \sum_{\substack{\text{ladder} \\ <i',j'>}}^{N_a} \boldsymbol{S}_{i'} \cdot \boldsymbol{S}_{j'} - g\mu_B B \sum_i^N S_i^z \tag{10}$$

Here N_c is the number of chains in the system, N_a is the number of atoms per chain and $N = N_a \times N_c$ is the total number of atoms in the system. Here only nearest neighbour interactions are significant. The chain summation indicates interactions of atoms in the chains, and the ladder summation indicates those for atoms from adjacent chains. J and J_c are the coupling constants between atoms in the chains and between the chains respectively. For this system both couplings will be anti-ferromagnetic, $J, J_c < 0$ with $J/k_B = -5$K and $J_c = 0.5J$ so that interactions between chains are significant enough to be considered in the system. Note that this Hamiltonian can easily be used to analyse the properties of molecular based spin ladders.[14,15]

The results the susceptibility of 2 atoms per chain are given in figure 15. Unsurprisingly, all susceptibilities behave like the even N systems that were discussed in Section 3.1. The susceptibility per atom is roughly the same in magnitude.

This is simply because the system has N_c 2 atom chains connected together by J_c, so the total susceptibility of each system is N_c times the 2 atom χ. The effects of the J_c coupling between chains reduce the χ slightly but the system is mainly dominated by 2 atom chain behaviour.

The susceptibilities for 3 atoms per chain shown in figure 16 are more interesting. It can be seen that the susceptibilities for odd N_c behave similarly to

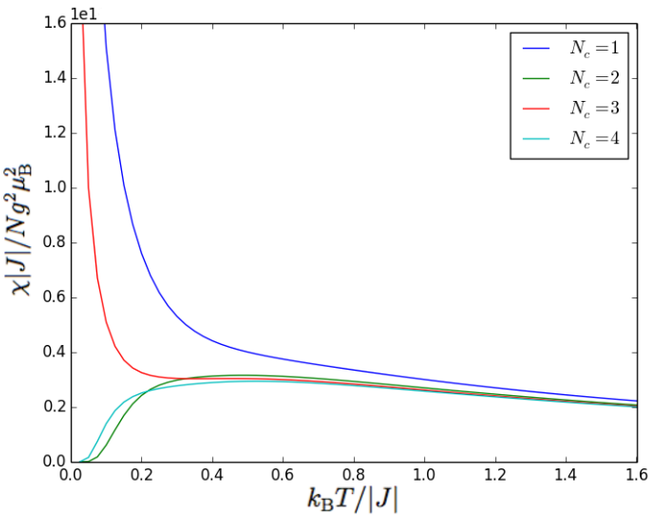

Figure 16: Magnetic susceptibility of layered systems with $1 - 4$ chains consisting of 3 atoms per chain, given in dimensionless units.

odd N systems in Section 3.1 but for even N_c the system has even N properties despite being a series of layered 3 atom chains. This is clearly due to the emergence of the field independent ground state, but it more constructive to consider figure 17 to understand how the physical structure affects the behaviour of the system.

The single chain will clearly behave as an odd N system as there are only 3 atoms. The 3 chain system contains 3 atom chains interacting vertically with coupling constant J, but also 3 atom chains interacting horizontally with coupling constant J_c. This gives a twofold contribution of odd atom chains to the system's properties.

The interesting case is for 2 chains since figure 17b shows that there are 3 atom chains vertically and 2 atom chains horizontally. This leads to the competing properties of the odd and even chains. Initially one would predict the odd chain behaviour to dominate since $J > J_c$, but this is clearly not the case as shown in figure 16.

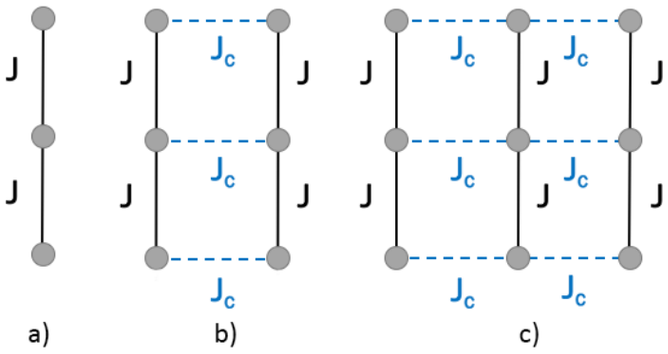

Figure 17: Layered system of 3 atoms per chain with coupling constants J and J_c a) single chain b) 2 chains c) 3 chains.

Similarly for 4 chains, the results in figure 16 indicates that the even chain behaviour dominates the susceptibilities despite there being more odd chains than even chains. This implies that even N inevitably leads to a $S = 0$ ground state energy with no B-field dependence. As a result the system will behave similarly to the even N rings in Section 3.1.

This behaviour only arises for these configurations because the coupling strength between the chains J_c is large enough to influence the system. The point at which J_c can be ignored can be found by evaluating a particular configuration, say $N_a = 3$ and $N_c = 2$, and varying its magnitude until the system no longer produces even chain behaviour.

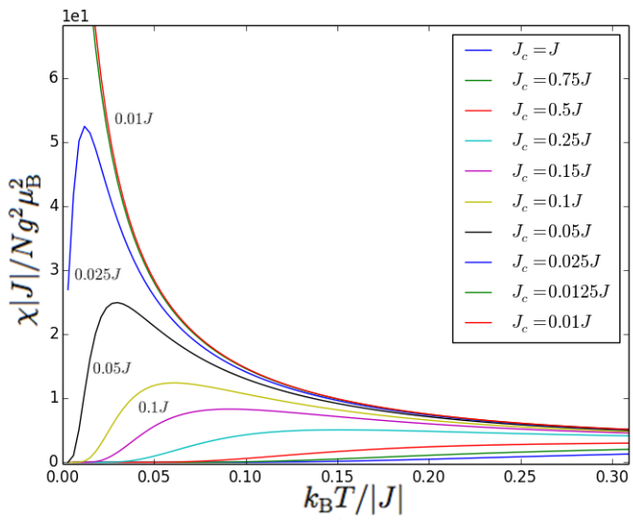

Figure 18: Magnetic susceptibility against temperature for a layered $N_a = 3$ $N_c = 2$ system with changing coupling J_c, given in dimensionless units.

Figure 18 shows that as J_c is reduced proportionally to J, the even chain effects become weaker and eventually allows the odd chain effects to dominate the total susceptibility. Although it stands to reason that odd N properties only fully dominate when the interactions between the chains are zero, $J_c = 0$. Even around the regions of $J_c \sim 0.01J$, at very low temperatures we can expect the curve to fall towards zero due to the presence of the $S = 0$ ground state. This illustrates the complexities of square lattice systems, as different configurations will produce different properties depending on the type of vertical and horizontal interactions taking place as well as the coupling strength J_c with respect to J.

4 Comparison of experimental data $CuCl_2(pyz)$

The comparison of experimental and theoretical results will confirm whether the Heisenberg model is appropriate for evaluating real magnetic systems. Organic molecules such as $CuCl_2(pyz)$ (pyz stands for the heterocyclic compound pyrazine) contain low dimensional magnetic behaviour that can approximated into a one dimensional chain.[16] The structure of $CuCl_2(pyz)$ is shown in figure 19. The Cu^{2+} ions are approximated as spin-$\frac{1}{2}$ particles which are joined by the organic pyrazine ligands to form a chain. The antiferromagnetic interactions in the chains are much stronger than those between the chains mediated by the Cl^- ions. Hence the interactions from the Cl^- ions can be safely ignored and the system can be modelled as a one dimensional chain (although we will see how this approximation breaks down at large temperatures).

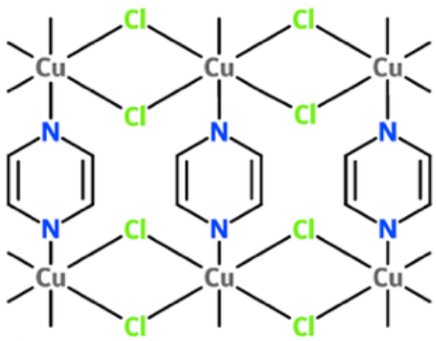

Figure 19: Structure of $CuCl_2(pyz)$ showing the Cu-pyz-Cu chains and Cu-Cl_2-Cu chains.[17]

The experimental susceptibilities of $CuCl_2(pyz)$ were obtained from SQUID magnetometry with a sample mass of $M = 13.3$mg, molecular mass of $M_m = 214.54 \text{gmol}^{-1}$ and density $\rho = 2.3869 \times 10^{-3}\text{gm}^{-3}$. The equation, $T_{max} = 0.64|J|/k_B$, from Bonner and Fisher[4] allows the coupling constant J to be calculated by finding the temperature T_{max} which gives the maximum susceptibility.

The experimental data gives a maximum susceptibility at $T_{max} = 16.999$K which leads to a coupling constant of $J/k_B = -26.56(2)$K with this method. This is a fairly good approximation to the experimental measurement $J_{exp}/k_B = -28(1)$K.[18]

The $CuCl_2(pyz)$ data is plotted in figure 20 alongside other approximations, where the coupling

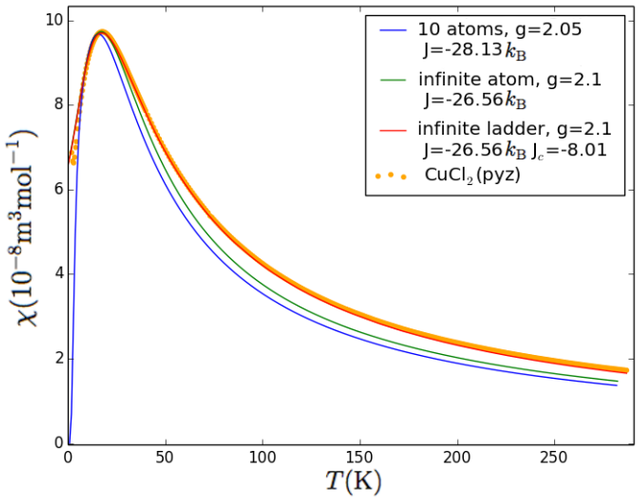

Figure 20: Magnetic susceptibility against temperature for experimental $CuCl_2$(pyz) data and the 10 atom chain, infinite chain and infinite ladder approximations given in real units.

J and Landé g-factor are altered to match experimental results. The results of the 10 atom chain are plotted against this data, where the conversion of susceptibility to units of $10^{-8}\mathrm{m}^3\mathrm{mol}^{-1}$ is given by

$$\chi = \frac{N_\mathrm{A} M}{\rho}\frac{\chi}{N}, \tag{11}$$

where N_A is Avogadro's number. Variations of J and g are made to match the 10 atom results with experimental data, this works best with $J/k_\mathrm{B} = -28.13(6)\mathrm{K}$ and $g = 2.05(4)$, which would otherwise deviate more from the experimental data if J_exp was used instead. This is clearly a bad approximation as the low temperature limits do not match and the data diverges at $T > 25\mathrm{K}$. The fact that $CuCl_2$(pyz) chains contain much more than 10 atoms points towards a more appropriate model.

The total number of atoms in the system is $N = N_A M/M_\mathrm{m} \sim 3.7 \times 10^{19}$. As shown in Section 3.1 as N increases they converge towards the infinite limit, so the infinite atom model from equation (7) is an intuitively better approximation for a $N \sim 3.7\times10^{19}$ system. The infinite atom model shown in figure 20 also uses the same conversion in equation (11). This uses the coupling $J/k_\mathrm{B} = -26.56(2)\mathrm{K}$ and g-factor $g = 2.1(1)$, which gives a very good approximation for low temperatures but the results still deviates at larger temperatures.

We assumed that the interactions from the Cl^- ions were negligible, although this is not necessarily the case at high temperatures where these interactions start to become more significant. This signals the need for a two dimensional model of $CuCl_2$(pyz),[18] such as the infinite ladder, which takes into account the interactions between the chains mediated by the Cl^- ions. This is given by[19]

$$\chi_\mathrm{L} = \frac{\chi_\infty}{1+\frac{4J_\mathrm{c}}{g^2\mu_\mathrm{B}^2}\chi_\infty}, \tag{12}$$

where χ_∞ is the susceptibility of the infinite chain and J_c is the coupling constant between the chains. The infinite ladder uses values $J/k_\mathrm{B} = -26.56(2)\mathrm{K}$, $g = 2.1(1)$ and $J_\mathrm{c}/k_\mathrm{B} = -8.01(5)\mathrm{K}$. The coupling between chains J_c is in good agreement with independent experiments,[18] where $J_{\mathrm{c\ exp}}/k_\mathrm{B} = -8(2)\mathrm{K}$. This is clearly a better approximation as the results do not diverge as much at high temperatures as shown in figure 20 and is much closer to the experimental data at both low and high temperature regions.

The infinite chain and infinite ladder results also indicate that the g-factor is actually closer to 2.1(1) which agrees with experimental measurements, $g_\mathrm{exp} = 2.1$.[20] This indicates that assuming the system can be modelled as purely spin-$\frac{1}{2}$ atoms is incorrect. There must be other factors that contribute to the total angular momentum have been ignored that influences the value of g. Nevertheless, these approximations are still very good and model the behaviour of $CuCl_2$(pyz) very well. This illustrates the effectiveness of the Heisenberg model for modelling the behaviour of complex magnetic molecules.

5 Conclusion

It can be seen that the Heisenberg model is extremely good for modelling molecular magnetic interactions, and coupling this with statistical mechanics proves to be extremely powerful for predicting the large scale properties. These theoretical models can be used to predict the behaviour of real molecular magnets with unique configurations and ionic interactions.

Different systems can be accounted for simply by imposing its boundary conditions on the Hamiltonian, where its properties can be found by manipulating the system's partition function. This project has involved the study of one dimensional systems such as the antiferromagnetic, ferromagnetic, alternating and anisotropic rings. Two dimensional systems were briefly examined by considering layered chains and comparison with experimental results were made with $CuCl_2$(pyz). The coupling constants and g-factor calculated were $J/k_\mathrm{B} = -26.56(2)\mathrm{K}$, $J_\mathrm{c}/k_\mathrm{B} = -8.01(5)\mathrm{K}$ and $g = 2.1(1)$, which are in good agreement with the experimental results, $J_\mathrm{exp}/k_\mathrm{B} = -28(1)\mathrm{K}$, $J_{\mathrm{c\ exp}}/k_\mathrm{B} = -8(2)\mathrm{K}$[18] and $g_\mathrm{exp} = 2.1$.[20]

Analysis of much larger and complex crystal structures (where $N \gg 12$) are limited by the fact that this requires the manipulation of $2^N \times 2^N$ matrices making the running of the programme impractical. Further study of larger systems can be made by using the Lanczos algorithm which works surprisingly well.[21,22] This reduces the dimensions of the matrices involved and approximations are

made to the partition function that implements the reduced energy eigenvalues.

This project has shown the effectiveness of the Heisenberg model in modelling such systems by making approximations to reduce the dimension of the system. Further study of complex structures will result in the development of computational methods, as it is essential to reduce the computational runtime for calculations of larger molecular systems.

Appendices

A Mathematical approximations

Many derivatives must be generated throughout this project, which by definition requires the infinitesimal change in the y variable over the infinitesimal change in the x variable. The finite difference is used, so evaluation of the change in these variables are made under small intervals. This is given by:

$$\frac{dy}{dx} = \frac{y(x+\delta x) - y(x)}{\delta x} \tag{13}$$

Where δx is a finite interval.

References

[1] W. Heisenberg and Z. Phys. **49**, pp. 619-636 (1928).

[2] L. J. de Jongh and A. R. Miedama, Adv. Phys. **23**, pp. 1-260 (1974).

[3] H. Kobayashi, T. Haseda and E. Kanda, J. Phys. Soc. **18**, 349 (1963).

[4] J. C. Bonner and M. E. Fisher, Phys. Rev. **135**, A640 (1964).

[5] Y. Savina, O. Bludov, V. Pashchenko, S. L. Gnatchenko, P. Lemmens and H. Berger Phys. Rev. B **84**, 104447 (2011).

[6] W. Duffy and K. P. Barr, Phys. Rev. **165**, 647 (1968).

[7] J. C. Bonner, H. W. J. Blöte, J. W. Bray and I. S. Jacobs, J. Appl. Phys. **50**, 1810 (1979).

[8] H. Manaka, I. Yamada and K. Yamaguchi, J. Phys. Soc. **66**, pp. 564-567 (1997).

[9] M. Eshel, A. Bino, I. Felner , D. C. Johnston, M. Luban and L. L. Miller, Inorg. Chem. **39** (7) (2000).

[10] M. Takahashi, Prog. Theor. Phys. **50** (5) pp. 1519-1536 (1973)

[11] W. Schottky, Physikalische Zeitsehrift **23**, pp. 448 (1992).

[12] P. Day, Phys. Scr. T. **49**, 729 (1993).

[13] J. Singleton, Rep. Prog. Phys. **63**, 1111 (2000).

[14] C. P. Landee, M. M. Turnbull, C. Galeriu, J. Giantsidis and F. M. Woodward, Phys. Rev. B **63**, 100402(R) (2001).

[15] B. Frischmuth, B. Ammon and M. Troyer, Phys. Rev. B **54**, R3714(R) (1996).

[16] T. Lancaster, S. J. Blundell, F. L. Pratt, M. L. Brooks, J. L. Manson, E. K. Brechin, C. Cadiou, D. Low, E. J. L. McInnes and R. E. P. Winpenny, J. Phys. Condens. Matter **16**, S4563 (2004)

[17] F. K. K. Kirschner, *Simulations of Low-Dimensional Antiferromagnetic Spin Systems*, Master's Thesis, University of Oxford (2015).

[18] R. T. Butcher, C. P. Landee, M. M. Turnbull and F. Xiao, Inorganica Chemica Acta, **361**, pp. 3654-3658 (2008).

[19] D. C. Johnston, Acta Physica Polonica A**91**, pp. 181-189 (1997).

[20] M. Inoue, S. Emori, K. Hara and M. Kubo, J. Magn. Reson. **17**, 212 (1975).

[21] J. Jaklic and P. Prelovsek, Phys. Rev. B **49**, 5065 (1994).

[22] J. Schnack and C. Heesing, Eur. Phys. J. B **86**, 46 (2013).